

Enzymatic and Free Radical Formation of *Cis*- and *Trans*- Epoxyeicosatrienoic *In Vitro* and *In Vivo*

Theresa Aliwarga^a, Brianne S. Raccor^b, Rozenn N. Lemaitre^c, Nona Sotoodehnia^{c,d}, Sina A. Gharib^e, Libin Xu^a, Rheem A. Totah^{a*}

^a Department of Medicinal Chemistry, University of Washington, Box 357610, Seattle, WA 98195, USA

^b Department of Pharmaceutical Science, Campbell University, PO Box 1090, Buies Creek, NC 27506, USA

^c Cardiovascular Health Research Unit, Department of Medicine, University of Washington, 1730 Minor Ave, Suite 1360, Seattle, WA 98101, USA

^d Division of Cardiology, University of Washington, Box 356422, Seattle, WA 98195, USA

^e Computational Medicinal Core, Center for Lung Biology, Division of Pulmonary & Critical Care Medicine, Department of Medicine, University of Washington, S376- 815 Mercer, Box 385052, Seattle, WA 98109, USA

E-mail addresses: tessa629@uw.edu (T. Aliwarga), raccor@campbell.edu (B.S. Raccor), rozenl@uw.edu (R.N. Lemaitre), nsotoo@uw.edu (N. Sotoodehnia), sagharib@uw.edu (S. A. Gharib), libinxu@uw.edu (L. Xu), rtotah@uw.edu (R.A. Totah)

*** Corresponding Author:** Rheem A. Totah, 206-543-9481 (Telephone), 206-685-3252 (Fax), rtotah@uw.edu.

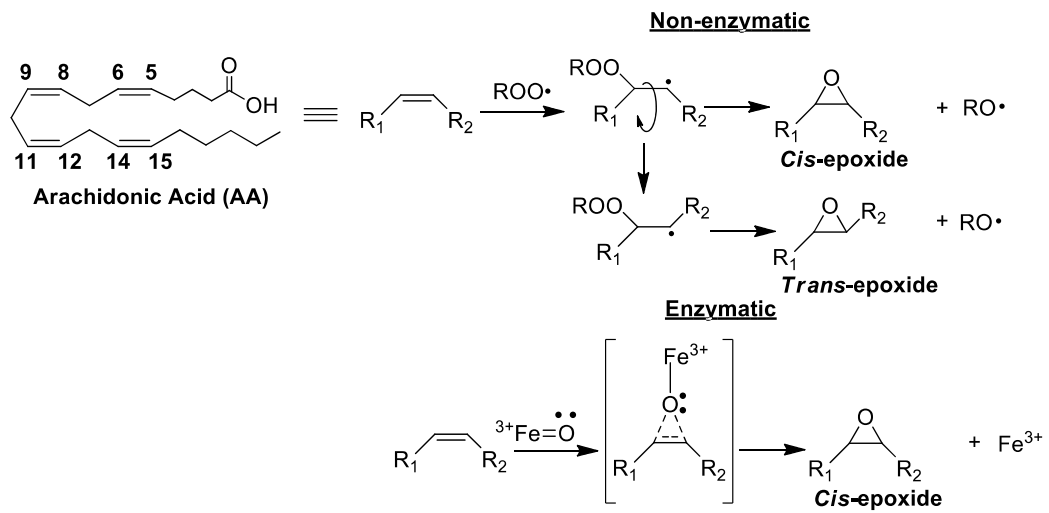
Abstract

Epoxyeicosatrienoic acids (EETs) are metabolites of arachidonic acid (AA) oxidation that have important cardioprotective and signaling properties. AA is an ω -6 polyunsaturated fatty acid (PUFA) that is prone to autoxidation. Although hydroperoxides and isoprostanes are major autoxidation products of AA, EETs are also formed from the largely overlooked peroxy radical addition mechanism. While autoxidation yields both *cis*- and *trans*-EETs, cytochrome P450 (CYP) epoxygenases have been shown to exclusively catalyze the formation of all regioisomer *cis*-EETs, on each of the double bond. In plasma and red blood cell (RBC) membranes, *cis*- and *trans*-EETs have been observed, and both have physiological functions. We developed a sensitive ultra-performance liquid chromatography tandem mass spectrometry (UPLC-MS/MS) assay that separates *cis*- and *trans*- isomers of EETs and applied it to determine the relative distribution of *cis*- vs. *trans*-EETs in reaction mixtures of AA subjected to free radical oxidation in benzene and liposomes *in vitro*. We also determined the *in vivo* distribution of EETs in several tissues, including human and mouse heart, and human and mouse RBC membranes. Formation of EETs in free radical reactions of AA in benzene and in liposomes exhibited time- and AA concentration-dependent increase and *trans*-EET levels were higher than *cis*-EETs under both conditions. In contrast, *cis*-EET levels were overall higher in biological samples. We propose a mechanism for the non-enzymatic formation of *cis*- and *trans*-EETs involving addition of the peroxy radical to one of AA's double bonds followed by bond rotation and intramolecular homolytic substitution ($S_{\text{H}}\text{i}$). Enzymatic formation of *cis*-EETs by cytochrome P450 most likely occurs via a one-step concerted mechanism that does not allow bond rotation. The ability to accurately measure circulating EETs resulting from autoxidation or enzymatic reactions in plasma and RBC membranes will allow for future studies investigating how these important signaling lipids correlate with heart disease outcomes.

Keywords

cis-EETs, *trans*-EETs, free radical oxidation, arachidonic acid, RBC, heart, CYP2J2

Graphical Abstract



1. Introduction

PUFAs are highly susceptible to free radical oxidation commonly known as lipid peroxidation. A comprehensive discussion of reactions involved in lipid peroxidation has been reviewed by Yin et al. [1]. Oxidative stress, associated with various disease states, perturbs the balance of reactive oxygen species (ROS), which in turn leads to increased lipid peroxidation. Briefly, the process originates in the formation of lipid radical followed by generation of lipid peroxy radical with molecular oxygen addition. The peroxy radical can propagate the chain reactions by either abstracting a hydrogen atom from another lipid molecule or adding to a double bond of another (Fig. 1). The radical formed after the addition tends to undergo intramolecular homolytic substitution ($S_{H\cdot}$) to give an epoxide and an alkoxyl radical that continues the chain reaction. Detailed mechanism of peroxy radical addition reactions has been discussed by Xu et al. [2]. Lipid peroxidation *in vivo* has been linked to the underlying pathophysiology of various disease states, including atherosclerosis, myocardial ischemia-reperfusion injury, diabetes, cancer, and neurodegenerative injury [3-7].

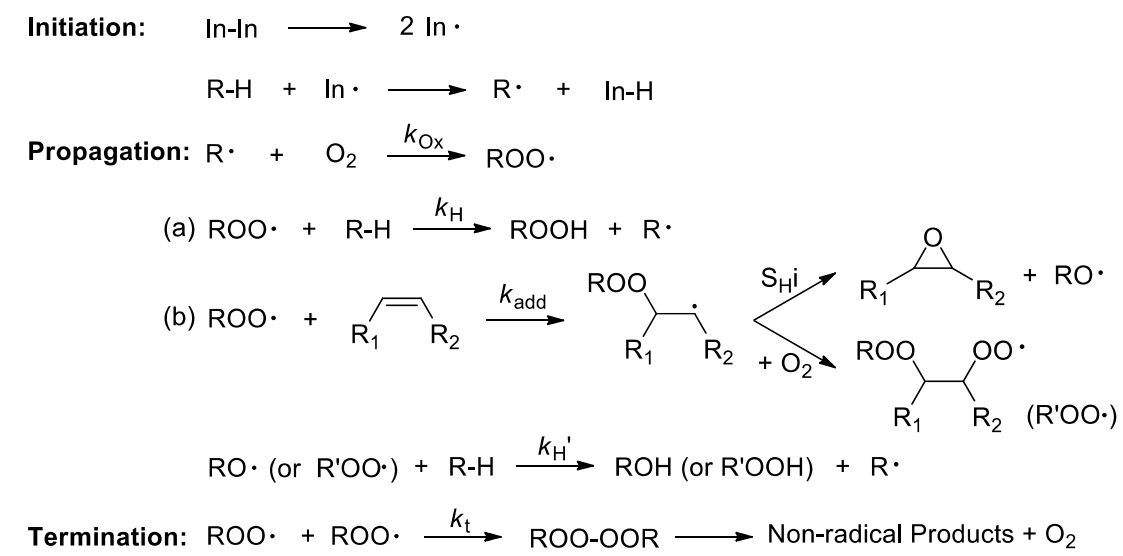


Fig 1. Free radical chain oxidation reaction and generation of epoxides by peroxy radical addition.

Abbreviations: EET, epoxyeicosatrienoic acid; AA, Arachidonic acid; PUFA, polyunsaturated fatty acid; UPLC-MS/MS, ultra-performance liquid chromatography tandem mass spectrometry; ROS, reactive oxygen species; NF- κ B, nuclear factor - κ B; RBC, red blood cell; *t*-AUCB, 4-[*trans*-4-[[tricyclo[3.3.1.1^{3,7}]dec-1-ylamino]carbonyl]amino]cyclohexyl]oxy]-benzoic acid (*t*-AUCB); MeOAMVN, 2,2'-azobis(4-methoxy-2,4-dimethylvaleronitrile); AIPH, 2,2'-azobis(2-(2-imidazolin-2-yl)propane) dihydrochloride; PBS, Dulbecco's phosphate buffered saline; TPP, triphenylphosphine; BHT, butylated hydroxytoluene (BHT); DETAPAC, diethylenetriaminepentaacetic acid; DLPC, 1,2-dilauryl-*sn*-glycero-3-phosphocholine; DOPC, 1,2-dioleoyl-*sn*-glycero-3-phosphocholine; n_{AA} , mole fraction of AA; n_{OA} , mole fraction of oleic acid; KPi, potassium phosphate; hydroxyeicosatetraenoic acid, HETE.

AA is an essential ω -6 PUFA found mainly esterified at the *sn*2-position of phospholipids. Like other PUFAs, AA is highly susceptible to lipid peroxidation leading to several compounds including hydroperoxides and isoprostanes [1]. Almost all products of AA autoxidation reported previously were derived from the hydrogen atom-transfer peroxidation mechanism due to the high reactivity of AA as a hydrogen atom donor at the *bis*-allylic position. However, limited information is available on the peroxy radical addition pathway during AA autoxidation, which is the focus of this report.

Release of AA from membranes is tightly regulated *in vivo* and is calcium-dependent. Upon activation of phospholipase A₂, AA is hydrolyzed from phospholipids and subject to oxidation through various pathways, including the CYP pathway (Fig. 2). It is well established that AA can be metabolized by various CYP isoforms to all regioisomers of physiologically active *cis*-EETs among other hydroxyl metabolites [8, 9]. EETs play several crucial roles especially in the cardiovascular system, including modulating vascular tone by activating calcium-sensitive potassium channels which in turn promotes hyperpolarization and relaxation of smooth muscle cells, attenuating inflammatory process by inhibiting pro-inflammatory transcription factor, nuclear factor- κ B (NF- κ B), and improving post-ischemic-reperfusion injury by enhancing ventricular repolarization recovery [10, 11].

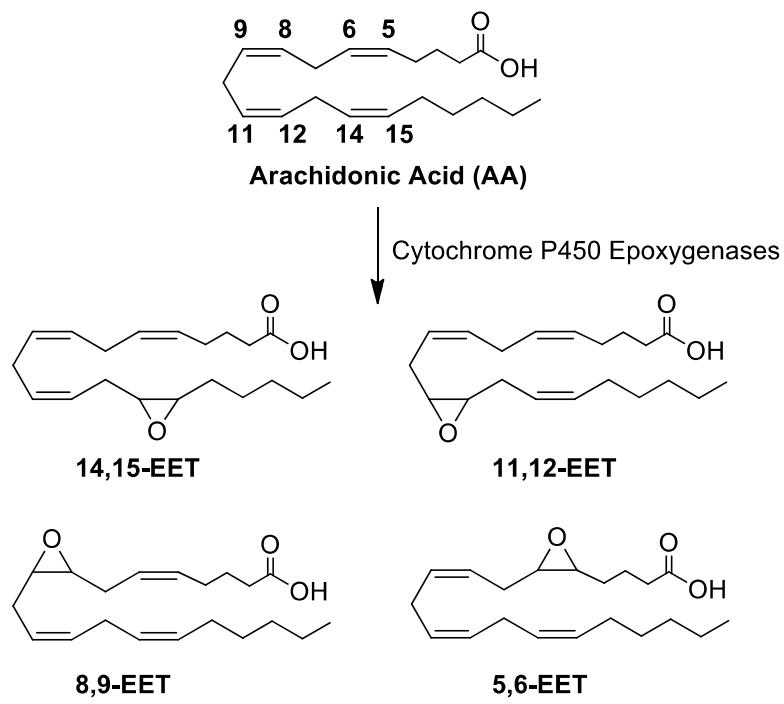


Fig. 2. AA metabolic pathway mediated by CYP epoxygenases to form all regioisomers of *cis*-EETs

Both *cis*- and *trans*-EETs detected in RBC membranes and plasma are mostly esterified in phospholipid membranes [12-14]. In fact, RBC membranes have been proposed to be a

reservoir of *cis*- and *trans*-EETs that can be formed either through CYP oxidation, by hemoglobin, or by free radical oxidation [13, 15, 16]. Like *cis*-EETs, *trans*-EETs are biologically active and have been shown to relax preconstricted rat arcuate arteries [14]. They are also hydrolyzed to dihydroxy metabolites at a much higher rate than *cis*-EETs by soluble epoxide hydrolase [13]. To date, the relative importance of *cis*- vs. *trans*-EETs in cardioprotection and their relative distribution in different biological samples have not been reported.

Here we developed an UPLC-MS/MS method capable of separating the *cis*- and *trans*-geometric isomers of all EET regioisomers and determined the product distribution of EETs formed through free radical oxidation in benzene and in liposomes *in vitro*. We also measured the *cis*- and *trans*-EETs distribution in several tissues *in vivo*, including mouse heart tissue and RBC, as well as human heart tissue and RBC. We further propose a mechanism for non-enzymatic formation of *cis*- and *trans*-EETs. Finally, *in vitro* CYP incubation conditions with AA were optimized using CYP2J2 as a model isozyme. ROS scavengers were varied to inhibit autoxidation of AA and more accurately determine CYP metabolite profile and product distribution.

2. Materials and Methods

2.1. Reagents

Stocks of AA, *cis*-EETs (14,15-, 11,12-, 8,9-, and 5,6-EETs), deuterated internal standards (14,15-EET-d₁₁, 8,9-EET-d₁₁, 5,6-EET-d₁₁, and 14,15-DHET-d₁₁) and 4-[[*trans*-4-[[tricyclo[3.3.1.1^{3,7}]dec-1-ylamino]carbonyl]amino]cyclohexyl]oxy]-benzoic acid (*t*-AUCB) were purchased from Cayman Chemical (Ann Arbor, MI). 2,2'-azobis(4-methoxy-2,4-dimethylvaleronitrile) (MeOAMVN) and 2,2'-azobis(2-(2-imidazolin-2-yl) propane) dihydrochloride (AIPH) were obtained from Wako Chemicals USA, Inc (Richmond, VA). Pure AA stocks were purchased from Nu-Chek-Prep, Inc (Elysian, MN). Dulbecco's phosphate buffered saline (PBS), ACS-grade ethyl acetate, chloroform, Optima-grade acetonitrile, water, and methanol were purchased from Fisher Scientific (Hampton, NH). Benzene, triphenylphosphine (TPP), butylated hydroxytoluene (BHT), phospholipase A₂ from *Naja mossambica mossambica*, pyruvic acid, and diethylenetriaminepentaacetic acid (DETAPAC) were obtained from Sigma-Aldrich (St. Louis, MO). 1,2-dilauryl-*sn*-glycero-3-phosphocholine (DLPC) and 1,2-dioleoyl-*sn*-glycero-3-phosphocholine (DOPC) were purchased from Avanti Polar Lipids, Inc (Alabaster, AL).

2.2. Free radical oxidation of AA in benzene

The total reaction volume was 200 μ L. Pure AA was reconstituted in benzene that was filtered through neutral alumina. The stock solution of AA (164.2 mM) was diluted in benzene to obtain 1, 10, 25, and 50 mM solutions. The reaction was then initiated with addition of MeOAMVN (10 μ L, 0.03 M) and incubated at 37°C in a sand bath for 1, 2, or 3 h. At the end of each time point,

the reaction was terminated by adding BHT (50 μ L, 0.2 M) and TPP (50 μ L, 0.2 M) in benzene at room temperature. For the zero-time point, the reaction was immediately terminated after addition of AA. Samples were cooled to room temperature and a 10 μ L aliquot was mixed with 10 μ L of internal standard solution (a mixture of d₁₁- 14,15-, 8,9-, 5,6-EETs and d₁₁-14,15-DHET in benzene, 3 μ g/mL each). Samples were dried under nitrogen at 25°C followed by reconstitution in 1 mL of 50% of water and 50% of 80:20 acetonitrile:methanol. Samples were then analyzed on the same day by LC-MS as described below.

2.3. Free radical oxidation of AA in liposomes

Free radical oxidation of AA in liposomes was achieved following a procedure by Xu et. al. [17]. Briefly, chloroform solutions of DLPC (20 μ L, 250 mM), of DOPC (n_{OA} 0 to 0.76), and of AA (n_{AA} 0 to 0.76) were mixed together so that the concentration of total fatty acyl chains remain constant. The mixtures were dried under nitrogen at 25°C and kept under vacuum for 10 min. The dried samples were reconstituted in PBS and sonicated for 20 sec. The suspension was incubated at 37°C for 10 min followed by another cycle of 20 second sonication. The free radical oxidation was initiated by addition of AIPH (10 μ L, 20 mM). Addition of BHT (50 μ L, 0.2 M) and TPP (50 μ L, 0.2 M) terminated the reaction at room temperature. After 30 min, internal standards (10 μ L, a mixture of d11- 14,15-, 8,9-, 5,6-EETs and d11-14,15-DHET in 1× PBS, 3 μ g/mL each) were added. The EETs were then extracted twice using nitrogen-purged ethyl acetate containing 0.1 mM TPP. The ethyl acetate extracts were combined and dried under nitrogen at 25°C. The dried residue was reconstituted using 1 mL of a solution containing 50% of water and 50% of 80:20 acetonitrile:methanol. The samples were then analyzed on the same day by LC-MS.

2.4. Mouse erythrocyte membranes and heart tissue

Adult C57BL/6 mice (N=8, 5 females and 3 males) were purchased from Charles River Laboratories. Whole blood from mice was collected through cardiac puncture following treatment with CO₂. The collected blood was washed three-times with cold 1× PBS and stored at -80°C until further processed. After removal of heart tissue from the chest cavity of the mouse, the tissue was immediately washed with cold 1× PBS and flash frozen in liquid nitrogen. All animal experiments were performed in compliance with approved protocols by Institutional Animal Care and Use Committee of the University of Washington.

2.5. Human erythrocyte membranes and heart tissue

Human erythrocyte membrane samples were from a repository of sudden cardiac arrest cases and population-based controls. In this study, we used a random sample of 28 control samples that had been collected between October 1988 and September 2005 as part of a case-control study of erythrocyte fatty acids and incident sudden cardiac arrest [18]. The University of Washington Human Subject Review Committee approved the study protocol. Discarded non-ischemic and

ischemic human heart residual tissues were obtained from University of Washington Medical Center as surgical waste during cardiac transplants and other procedures. Ventricular tissues were immediately flash-frozen in liquid nitrogen and stored at -80°C until further processing.

2.6. Extraction of EETs from erythrocyte membranes

Methods to extract RBC and cardiac tissue EETs were adapted from published protocols [12, 19]. Each tissue was extracted as duplicate samples. Briefly, for erythrocyte membranes, 0.5 mL of deionized water and 10 µL of internal standard (a mixture of d₁₁- 14,15-, 8,9-, 5,6-EETs and d₁₁-14,15-DHET, 3 µg/mL each) were added to 0.5 mL of RBC membranes containing 50 mg/mL total protein for human and 30 mg/mL total protein for mouse. The samples were centrifuged at 3,500 rpm for 5 min at 4°C. The RBC samples were extracted using 4 mL of 2:1 chloroform:methanol containing 0.1 mM TPP, followed by rotary mixing for one hour at 4°C. The mixture was then centrifuged at 3,500 rpm for 15 minutes at 4°C to remove cellular debris. The chloroform layer was dried under nitrogen at 25°C, followed by addition of 50 mM Tris-HCl, 100 mM NaCl, 1 mM CaCl₂ buffer, pH 9.2 containing 10 units of phospholipase A₂ from *Naja Mossambica Mossambica* (1 mL). The samples were incubated for 30 minutes at 37°C to hydrolyze EETs from the membrane. The EETs were extracted twice with nitrogen-purged ethyl acetate containing 0.1 mM TPP (2 × 2mL), and the ethyl acetate fractions were pooled and evaporated to dryness under nitrogen at 25°C. The lipid residue was reconstituted in 10 µL of DMSO to ensure complete dissolution of EETs and 40 µL of a solution containing 50% of water and 50% of 80:20 acetonitrile:methanol, respectively. The samples were then analyzed directly by LC-MS.

2.7. Extraction of EETs from cardiac tissue

EET extraction from cardiac tissue was initiated by homogenizing the cardiac tissue in 0.5 mL of cold 1× PBS in the presence of 12.1 µM *t*-AUCB, a soluble epoxide hydrolase inhibitor, and six ceramic beads using Precellys24 (Bertin Instruments, Rockville, MD) at 6800 rpm for 6 × 30 seconds with 60 seconds delay between cycles. Prior to dividing the homogenized tissue into duplicate aliquots of 150 µL, 10 µL of internal standards (a mixture of 14,15-EET-d₁₁, 8,9-EET-d₁₁, 5,6-EET-d₁₁, and 14,15-DHET-d₁₁, 3 µg/mL each) were added to each sample of the homogenized tissue. The rest of the EET extraction protocol from the cardiac tissue followed similar procedure for EET extraction from RBC above. All extractions were performed in duplicates.

2.8. In vitro incubation using reconstituted CYP enzyme system

In vitro experiments were performed using recombinantly expressed and purified CYP2J2 [20]. Reconstituted enzyme system consisted of purified CYP2J2 (25 pmol), cytochrome P450 reductase, and cytochrome b5 in a ratio of 1:2:1, respectively in 50 µg/mL of extruded DLPC (500 µL total incubation volume). The buffer was 100 mM potassium phosphate buffer, pH 7.4

containing 0.1 mM DETAPAC. Following addition of NADPH (1.0 mM), the samples were pre-equilibrated at 37°C for 3 min after which the reaction was initiated with 50 µM AA containing 1 mM pyruvate. After 30 minutes, reactions were terminated with 2 mL of nitrogen-purged ethyl acetate containing 0.01% BHT to minimize non-enzymatic AA oxidation and a mixture of internal standards (1 µg/mL of 14,15-EET-d₁₁, 8,9-EET-d₁₁, and 5,6-EET-d₁₁ 3 µg/mL each) was added. The quenched reactions were vortexed rigorously for 10 minutes followed by centrifugation at 3500 rpm at 4°C for 5 min. The ethyl acetate extraction was performed twice, the organic layers were combined and evaporated to dryness under a gentle stream of nitrogen at room temperature. The residue was reconstituted with 10 µL of DMSO and 40 µL of a solution containing 50% of water and 50% of 80:20 acetonitrile:methanol, respectively. Samples were analyzed using LC-MS-MS on the same day.

2.9. Liquid chromatograph and mass spectrometric assay to quantify EETs

Quantification of *cis*- and *trans*-EETs was performed on a Waters Xevo TQ-S triple quadrupole mass spectrometer operated in negative ion mode electrospray coupled to a Waters UPLC. The EETs were separated on a Waters Acquity UPLC® BEH Shield RP C18 1.7 µm, 100 x 2.1 mm column with the mobile phase water containing 0.05% acetic acid (solvent A) and 80:20 acetonitrile: methanol containing 0.05% acetic acid (solvent B). The various isomers of EETs were separated using the following gradient: solvent B was held at 62% from 0 to 5.5 min, then held at 55% from 5.5 to 6 min, followed by an increase to 58% from 6 to 18 min, and finally increased to 100% from 18.1 to 19.1 min. Solvent B was then held at 62% from 20 to 23 min to re-equilibrate the column. Flow rate was constant at 0.3 mL/min throughout the run. For the first 2 min of runtime, 100% of the flow was diverted into waste. The MS conditions were the following: capillary voltage 2 kV, cone voltage 20 V, source temperature 150°C, desolvation temperature 450°C. The mass transitions that were monitored are 319.1 > 219.1 (14,15-EET), 319.1 > 208 (11,12-EET), 319.1 > 166.7 (11,12-EET), 319.1 > 155.1 (8,9-EET), 319.1 > 191.2 (5,6-EET) and compared to their corresponding deuterated standards. For 11,12-EET, 14,15-EET-d₁₁ was used as the internal standard.

In the absence of authentic standards, *trans*-EETs were identified based on retention time, fragmentation pattern and comparison to methods previously published [15]. To further confirm the presence and identity of *trans*-EETs, a free radical oxidation sample that contained 50 mM AA and oxidized for 3 hours in liposomes was analyzed using High Resolution/High Mass Accuracy Thermo LTQ-OrbiTrap, which confirmed the identity of the peaks presumed as *trans*-EETs came from the same parent ions and had the same fragmentation patterns as their corresponding *cis*-EET (Fig. S1).

2.10. Data analysis

Mass spectrometry data were analyzed using MassLynx 4.1. Data analysis was performed using Prism 5.04 (GraphPad, La Jolla, CA). In the free radical oxidation study, experiments were

performed in triplicates and reported as the means \pm S.D. Mass transition 319.1>208 was used to obtain peak area ratio for 11,12-EET. Experiments measuring EETs from biological samples were reported as means \pm standard deviations.

Integrated peak area of each analyte was normalized to the corresponding peak area of internal standard. In addition to analyte normalization to its internal standard, the normalized peak areas of each analyte at the zero time point were subtracted from the corresponding peak areas of each sample.

In optimization of *in vitro* incubation using reconstituted CYP enzyme system, experiments were performed in duplicates. In this subset of data, peak height of analyte, instead of peak area, was used and further normalized to its internal standard. As mentioned above, two mass transitions were monitored for 11,12-EET; 319.1>166.7 and 319.1>208. The peak intensity of 11,12-EET at 319.1>166.7 was higher than 319.1>208 even though chromatographic separation between 11,12-EET and 8,9-EET at mass transition 319.1>166.7 was not at baseline level. Peak height was used to quantitatively measure 11,12-EET for another set of experiment. The percentage of non-NADPH-dependent EETs was obtained by taking ratio of the normalized peak height of no-NADPH control and the normalized peak height of corresponding sample that contained NADPH.

3. Results

3.1 Free radical oxidation of AA in benzene or liposomes leads to formation of both *cis*- and *trans*- EETs

Free radical oxidation of AA at various concentrations (ranging from 1 to 50 mM) was initiated by MeOAMVN at 37 °C and the formation of *cis*- and *trans*- EETs was monitored at different time points using UPLC-MS/MS. In addition to the major hydroxyl metabolites, both *cis*- and *trans*-EETs were formed in this reaction (Fig. S2). Formation of *cis*- and *trans*- EETs was linear with respect to time- and AA concentration for all regioisomers with Fig. 3A-D demonstrating this relationship for 14,15-EET and Fig. S3-S4 showing all other regioisomers. Furthermore, for all conditions, *trans*-EETs formation was favored over *cis*-EETs formation by approximately 1.7 to 5.1 fold (Fig. 3E, Fig. 4A, and Fig S5). The percentage of each isomer of EET (regio- or stereo- isomer) to total EETs formed remained relatively constant at different AA concentrations and various time points as summarized in Table 1.

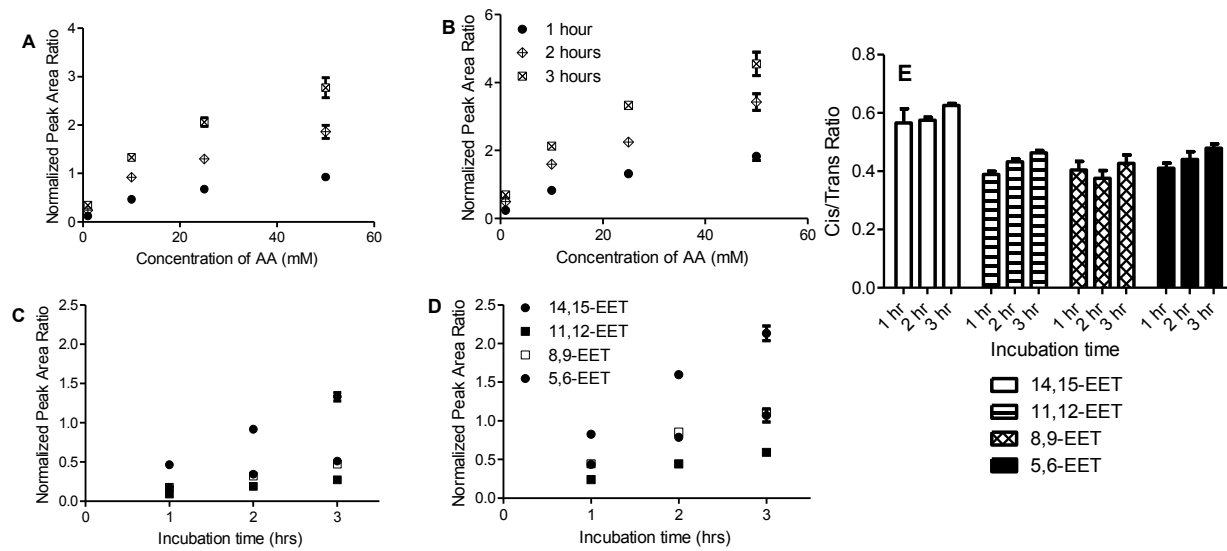


Fig. 3. Concentration- and time-dependent formation of non-enzymatic EETs and ratio of cis-/trans-EETs from AA in benzene. Concentration-dependent formation of non-enzymatic (A) *cis*-14,15-EET, (B) *trans*-14,15-EET. Time-dependent formation of non-enzymatic (C) *cis*-EETs, (D) *trans*-EETs at 10 mM AA. (E) Ratios of *cis*- to *trans*-EETs in benzene in the presence of 10 mM AA at various incubation time points remain unaltered. For this subset of experiments, each time point reaction was performed in triplicates and normalized to its zero-time point. Each data point shows mean \pm S.D.

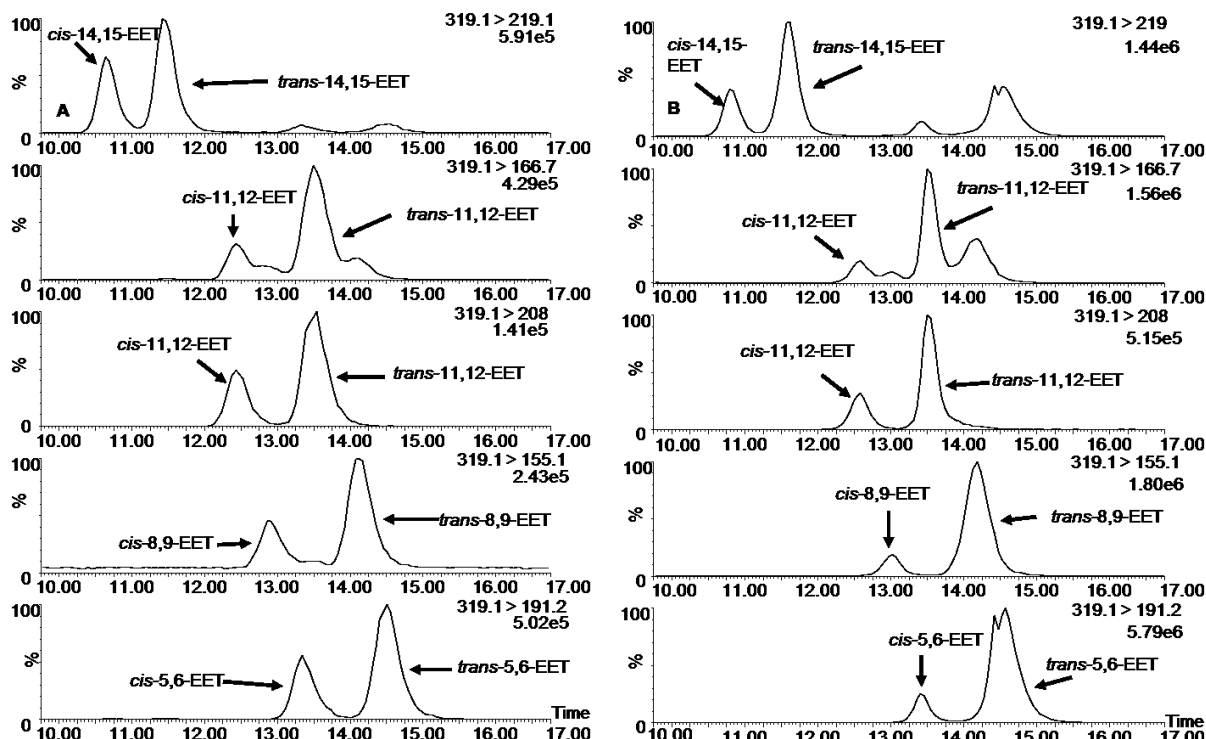


Fig. 4. Extracted ion chromatograms of EETs formed during free radical oxidation in benzene (A) and liposomes (B). The chromatograms demonstrate separation of *cis*- and *trans*-EETs. The levels of *trans*-EETs are higher than the level of *cis*-EETs during free radical oxidation.

Table 1. Percentages of each *cis*- and *trans*-EET relative to total *cis*- or *trans*-EETs, respectively, in benzene and liposomes

Reaction condition		% 14,15-EET	% 11,12-EET	% 8,9-EET	% 5,6-EET
Benzene	<i>cis</i> -	51 ± 2	11 ± 1	19 ± 1	19 ± 3
	<i>trans</i> -	43 ± 4	12 ± 1	22 ± 2	21 ± 3
Liposomes	<i>cis</i> -	28 ± 5	9.1 ± 2	27 ± 4	36 ± 9
	<i>trans</i> -	18 ± 3	5.1 ± 0.8	32 ± 3	45 ± 6

Each entry is an average of four concentrations and three time points. Experiments were performed in triplicates and data are presented as mean ± S.D.

To study radical formation of EETs in a more physiologically relevant system, oxidation of AA was performed in liposomes. The reaction contained a constant mole fraction of DLPC while varying mole fractions of oxidizable phospholipid, DOPC, and AA, so that the total moles of fatty acyl chain remains constant in the incubation. Free radical oxidation was initiated with water-soluble radical initiator, AIPH, at 37°C. Similar to radical reactions in benzene, *cis*- and *trans*-EETs formation was linear with time- and mole fraction of AA in liposomes for all regioisomers. The linear formation of 14,15-EET is shown as an example in Fig. 5A-D with other regioisomers shown in Fig. S6 and Fig. S7. The ratio of each regioisomer of EET relative to total EETs remained unchanged for both *cis*- and *trans*-EETs at various concentrations of AA and at various time points (Fig. 5E and Fig S8). The formation of *trans*-EETs was also favored in liposomes by approximately 2.6 and 8.4 over *cis*-EETs formation, even more so than those in solution oxidation (Fig. 5E, Fig. 4B, and Fig. S8). Compared to free radical oxidation in solution (i.e. benzene), more variability was observed in reactions in liposomes. At 1 mM of AA (n_{AA} of 0.015), the levels of both *cis*- and *trans*-EETs were similar to those observed in benzene. However, the formation of EETs in the presence of liposomes at higher concentration of AA was more efficient than in benzene as seen in Fig. 5A-B and Fig. S6-S7. Regardless of the difference in product distribution between benzene and liposome oxidations, the percentages of each regioisomer of EETs relative to total EETs was also relatively unaltered across all conditions (concentration and time) in liposome as seen in Table 1 (Bottom half).

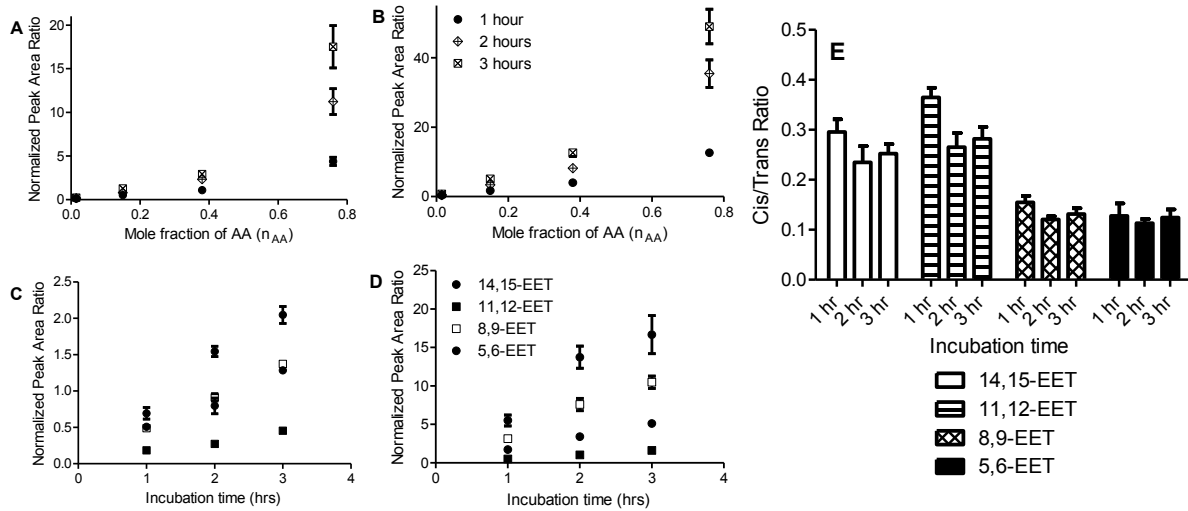


Fig. 5. Mole fraction- and time-dependent formation of non-enzymatic EETs and ratio of *cis*-/trans-EETs from AA in liposomes. Mole fraction-dependent formation of non-enzymatic (A) *cis*-14,15-EET, (B) *trans*-14,15-EET. Time-dependent formation of non-enzymatic (C) *cis*-EETs, (D) *trans*-EETs at n_{AA} of 0.15. (E) Ratios of *cis*- to *trans*-EETs in liposomes at various incubation time points and at n_{AA} of 0.15 did not change significantly. For this subset of experiment, each time point reaction was performed in triplicates and normalized to its zero time point. Each data point shows mean \pm S.D.

3.2. Product distribution of *cis*- and *trans*- EETs in biological samples

Extraction of EETs from erythrocyte membranes of C57BL/6 mice and humans revealed the presence of both geometric isomers of all EET regioisomers (Fig. 5). In contrast to the free radical oxidation reactions, *cis*-EETs are higher than *trans*-EETs in erythrocyte membranes as evidenced by the larger normalized peak-height ratios in Table 2 and 3. The ratios of *cis*-/*trans*-EETs for each regioisomer from mouse RBC membranes ranged from 1.0 to 2.4 (N=8), while the ratios from human RBC membranes ranged from 1.0 to 3.1 (N=28). For each EET pair, the *cis*-/*trans*- ratios in RBC membranes of both mouse and human are very similar.

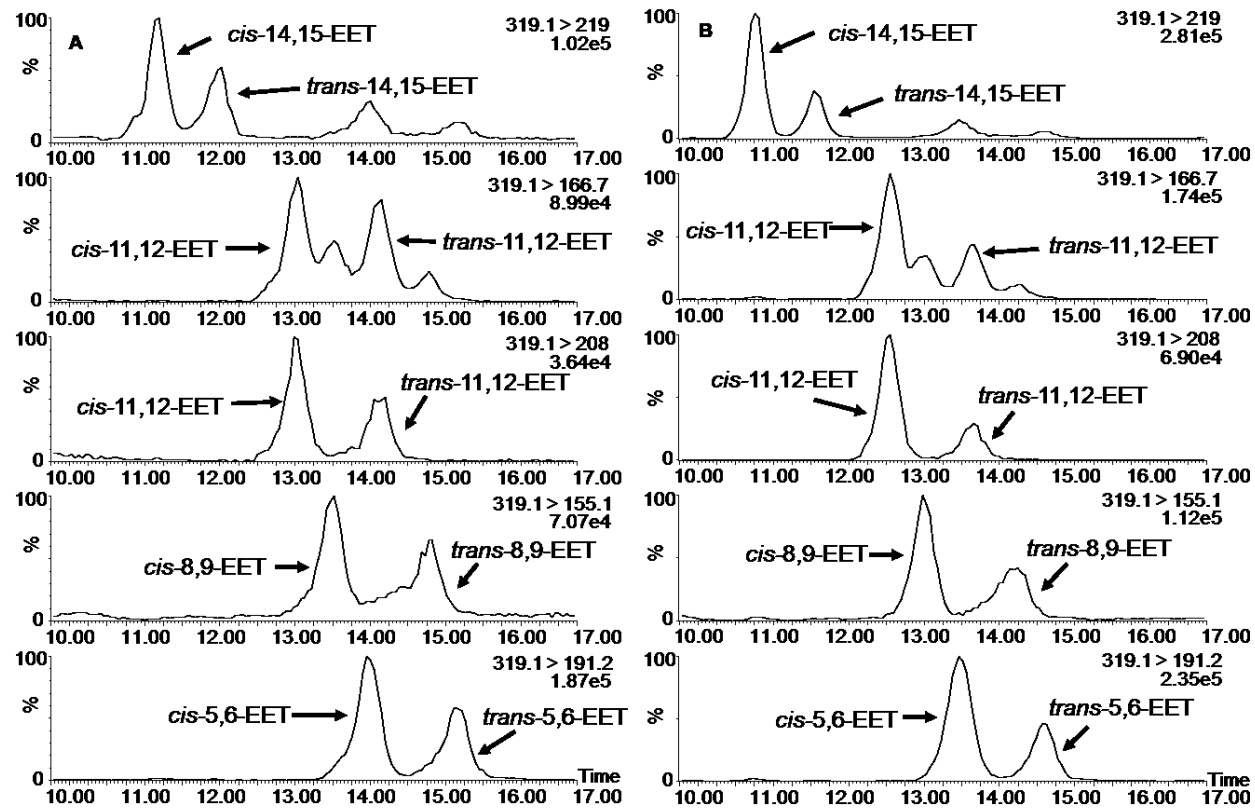


Fig. 6. Extracted ion chromatograms of EETs extracted from erythrocyte membrane of C57BL/6 mice (A) and human (B). The chromatograms demonstrate separation of *cis*- and *trans*-EETs. The levels of *cis*-EETs are generally higher than the level of *trans*-EETs in erythrocyte membranes in both mice and humans.

The ratios of *cis*-/*trans*-EETs for each regioisomer from mouse heart tissues ranged from 0.38 to 1.3 (N=8), while the ratios from human RBC membranes ranged from 0.80 to 2.8 (N=12). In mouse heart tissues, the levels of *cis*-14,15- and *cis*-5,6-EETs were similar to their *trans*-EETs while the levels of *cis*-11,12- and *cis*-8,9-EETs were significantly lower than their *trans*-counterparts (Table 2). In diseased human heart tissues, the levels of all *cis*-EETs were higher than their corresponding *trans*-EETs (Table 3).

Table 2. Normalized peak height ratios and ratios of each *cis*- and *trans*-EET in mouse RBC membranes and hearts

	Mouse RBC (N=8)			Mouse Heart(N=8)		
	<i>cis</i> -	<i>trans</i> -	<i>cis</i> -/ <i>trans</i> -	<i>cis</i> -	<i>trans</i> -	<i>cis</i> -/ <i>trans</i> -
14,15-EET	0.013 ± 0.003	0.0065 ± 0.002	2.1 ± 0.3	0.0031 ± 0.0005	0.0026 ± 0.0004	1.2 ± 0.1
11,12-EET	0.015 ± 0.004	0.012 ± 0.004	1.4 ± 0.4	0.0032 ± 0.0006	0.0041 ± 0.0008	0.77 ± 0.07
8,9-EET	0.0055 ± 0.0007	0.0036 ± 0.001	1.7 ± 0.6	0.0023 ± 0.0004	0.0054 ± 0.001	0.43 ± 0.05
5,6-EET	0.0054 ± 0.001	0.0039 ± 0.001	1.5 ± 0.5	0.0017 ± 0.0003	0.0017 ± 0.0004	1.0 ± 0.2

Mouse RBC membranes were normalized to 30 mg/mL of total protein while mouse heart tissues were normalized to weight. The data in the table are presented as means ± S.D.

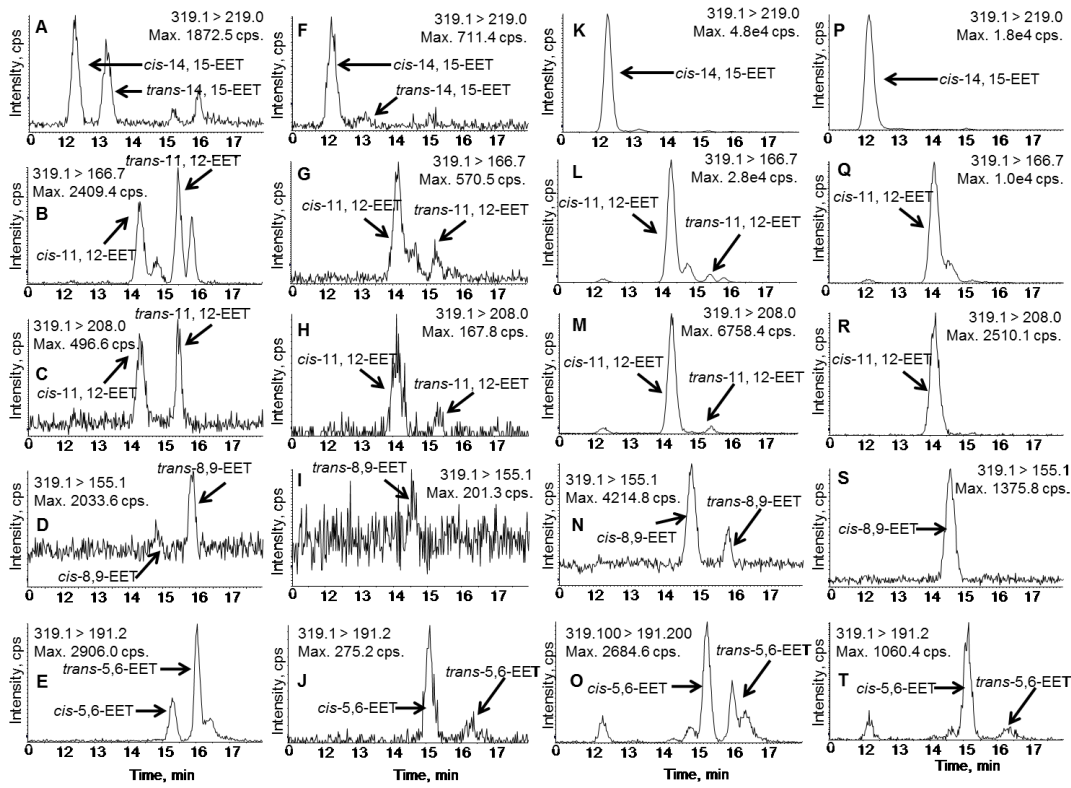
Table 3. Normalized peak height ratios and ratios of each *cis*- and *trans*-EET in human RBC membranes and diseased hearts

	Human RBC (N=28)			Human Heart (N = 12)		
	<i>cis</i> -	<i>trans</i> -	<i>cis</i> -/ <i>trans</i> -	<i>cis</i> -	<i>trans</i> -	<i>cis</i> -/ <i>trans</i> -
14,15-EET	0.0033 ± 0.001	0.0019 ± 0.001	2.0 ± 0.6	0.00066 ± 0.0001	0.00038 ± 0.0001	1.9 ± 0.6
11,12-EET	0.0026 ± 0.001	0.0021 ± 0.001	1.5 ± 0.5	0.0011 ± 0.0003	0.0011 ± 0.0004	1.2 ± 0.4
8,9-EET	0.0032 ± 0.001	0.0020 ± 0.001	1.9 ± 0.6	0.0022 ± 0.0005	0.0010 ± 0.0003	2.3 ± 0.5
5,6-EET	0.0028 ± 0.002	0.0015 ± 0.001	2.2 ± 0.9	0.0018 ± 0.0008	0.0011 ± 0.0004	1.7 ± 0.6

Human RBC membranes were normalized to 50 mg/mL of total protein while heart tissues were normalized to tissue weight. The data in the table are presented as means ± S.D.

3.3. In vitro enzymatic and non-enzymatic formation of *cis*- and *trans*- EETs

CYP2J2 was chosen as a model CYP epoxygenase since it is capable of generating all regioisomers of *cis*-EETs and at approximately similar amounts [21]. In a CYP2J2 reconstituted system including cytochrome P450 oxidoreductase and cytochrome b5, both *cis*- and *trans*- regioisomers of EETs were observed in the presence and absence of NADPH (Fig.7), suggesting contribution from both enzymatic and autoxidation processes. We sought to establish conditions that would diminish, if not eliminate, the non-NADPH dependent formation of EETs during CYP incubations to facilitate accurate metabolite identification and kinetic studies of various fatty acids. Thus, we investigated the effect of an iron-chelating agent, DETAPAC, and hydrogen peroxide scavenger, pyruvate, at various concentrations. Table 4 shows percentage of remaining EETs that were formed in non-NADPH-dependent manner in the presence of each protective reagent. Spectrometric binding studies were conducted and confirmed that neither pyruvate or DETAPAC bind to the CYP2J2 active site and had no effect on the iron spin state (data not shown).



Components					
KPi	+		+		+
DETAPAC	-		+		+
Pyruvate	-		+		+
NADPH	-		-	+	+

Fig. 7. Extracted ion chromatograms of reconstituted CYP enzyme incubation of AA in the absence and presence of NADPH, DETAPAC, and pyruvate. Formation of non-NADPH-dependent *cis*- and *trans*-EETs was observed at greater intensity in the no NADPH control in potassium phosphate (KPi) buffer (A-E) while addition of DETAPAC and pyruvate markedly reduced NADPH-independent formation of EETs (F-J). In the presence of NADPH and absence of both DETAPAC and pyruvate, *cis*-EETs were observed at a very high level, which confirmed that CYP exclusively make *cis*-EETs (K-O). In this sample, *trans*-EETs were still observed. Reducing non-NADPH-dependent formation of EETs ensures the formation of observed EETs was mediated by CYP catalysis. Addition of DETAPAC and pyruvate markedly diminished the formation of non-NADPH-dependent EETs (P-T). Normalization of EETs formed in the incubation to its corresponding no NADPH control was still necessary for all samples.

Table 4. Percent remaining of NADPH independent formation of EETs in reconstituted CYP enzyme system according to materials and methods.

Additives	14,15-EET	11,12-EET	8,9-EET	5,6-EET
EDTA	10.3%	14.2%	25.1%	56.3%
DETAPAC	6.5%	9.2%	15.9%	61.9%
EDTA + Pyruvate	4.8%	7.4%	12.2%	29.9%
DETAPAC + Pyruvate	3.2%	4.7%	6.9%	21.3%

Each condition was performed in duplicates.

4. Discussion

EETs have been implicated in many biological processes and play an important role in cardioprotection. We sought to determine the contribution of autoxidation to the formation of *cis*- and *trans*-EETs both in benzene and in liposomes, a more physiologically relevant system. The key finding of this study is that EETs are readily formed from AA under free radical oxidation conditions. All regio- and geometric- isomers were formed. The percentage of each *cis*- or *trans*-EET to total EETs did not change with increasing concentration of AA or with time whether reactions were carried out in benzene or liposomes. However, the percentages of both *cis*- and *trans*-14,15- and 5,6-EETs were significantly different between solution and liposome reactions. Formation of 14,15-EET appeared to be less favored in liposomes than in solution while the formation of 5,6-EET seemed to be more favored in liposomes. It is possible that the heterogeneous environment of liposomes contributes to 5,6-EET formation. The double bond at the C5 position is much closer to the carboxylic acid group than double bond at the C14 position. In the presence of liposomes, AA would be more likely to bury its hydrophobic tail; therefore, access to the double bond at the C14 position would be slightly restricted by lipid peroxy radicals and oxidation will be more favorable at the 5,6-position. Similar regio-distribution of oxidation products of linoleic acid in liposomes has been reported previously, where formation of C9-isomers are preferred over C13-isomers [17].

The ratios of *cis*- to *trans*-EETs from free radical oxidation are in general higher in benzene than in liposomes as shown in Figures 3E and 5E. Irrespective of the reaction medium, formation of *trans*-EETs was favored over *cis*-EETs. In contrast, levels of *cis*-EETs were, in general, either more favored or similar to *trans*-EETs depending on the specific regioisomer pairs in biological samples, such as human and mouse RBC membranes or human and mouse heart tissues. Of note, a considerably higher ratio of *cis*-/*trans*-8,9-EETs was observed in human heart tissues compared to mouse (Tables 2 and 3). This may be due to the diseased nature of the human heart tissue available to us, compared to healthy mouse tissue. However, further studies using healthy human heart tissue will be necessary to confirm this observation. Presence of all *cis*- regioisomer of EETs in human RBC membranes was shown by Nakamura et al., but the authors did not report the presence of both *cis* and *trans* in that publication [15]. In the analytical method developed in this study, both the *cis*- and *trans*-EETs present in RBC membranes were easily resolved (Fig. 6), which enabled their detection for the first time. While we clearly demonstrated that both geometric isomers of EETs are observed in the RBC membranes of mouse and human, their origin is less certain. EETs, both *cis*- and *trans*-, could potentially result from various sources, including enzymatic CYP or hemoglobin oxidation of hydrolyzed AA, or free radical oxidation of either free AA or AA esterified to phospholipids in the membrane.

CYP epoxygenases are known to only form *cis*-EETs (Fig. 7K-T) while autoxidation of AA leads to formation of both *cis*- and *trans*-EETs with preference to *trans*-regioisomers (Fig. 7A-E) [8,9]. The most likely mechanism of *trans*-EETs formation is through a peroxy radical addition mechanism. Peroxy radical addition to any of the double bonds of AA leads to the formation of a carbon radical, which could directly undergo S_{H1} reaction to give the *cis*-EETs, or undergo S_{H1} after rotation of the σ bond to give the *trans*-EETs as proposed in Fig. 8.

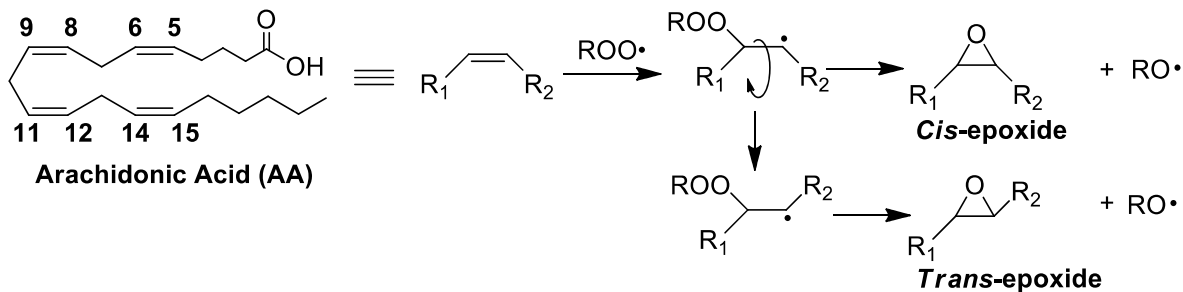


Fig. 8. Proposed mechanism of *cis*- and *trans*-EET formation via free radical oxidation.

Another potential mechanism is the *cis*-*trans* isomerization of AA prior to free radical oxidation or enzyme catalysis. Roy et al. reported that certain *trans* double bonds of AA lead to formation of *trans*-EETs in CYP-catalyzed reactions [22]. The process of *cis*- to *trans*- AA isomerization can be mediated by nitrogen dioxide, a free radical byproduct of nitric oxide and nitrite oxidation or thiyl radicals [23,24]. However, these mechanisms are unlikely to occur under *in vitro* reaction conditions. On the other hand, in CYP-mediated reactions, the iron-oxo

species (or potentially the hydroperoxy species) catalyzes the epoxide formation in a one-step concerted mechanism that does not allow for bond rotation and formation of *trans*-EETs [25].

Owing to the fact that EETs are formed from autoxidation of AA, it is important to optimize *in vitro* CYP incubation conditions to minimize the contribution from autoxidation. This will ensure that formation of *cis*-EETs observed in the presence of NADPH are mediated exclusively by CYP catalysis. Thus, we tested several approaches to minimize autoxidation without affecting enzymatic activity. In *in vitro* systems, non-NADPH-dependent EETs are potentially generated from Fenton chemistry. Therefore, addition of iron-chelating agents, EDTA or DETAPAC, markedly inhibited the formation of EETs from autoxidation. Another major uncoupling product of CYP catalysis is hydrogen peroxide, which can initiate the P450 cycle and also lead to EETs formation. To circumvent this reaction, pyruvate was also added to scavenge hydrogen peroxide [26]. Combination of both, iron-chelating agent and pyruvate efficiently inhibited the majority of EETs formation from autoxidation as shown in Table 4. In addition, all incubations were performed in the dark to avoid photoxidation and all analyses by UPLC-MS/MS were performed immediately following quenching of reactions to minimize oxidation and degradation of metabolites.

Lipid peroxidation is involved in the pathophysiology of various human disorders including cardiovascular disease. Oxidative stress during these disease states leads to the increase of reactive oxygen species, which increases lipid peroxidation due to the susceptibility of PUFAs to oxidation. Autoxidation of AA has been previously reported to form hydroperoxides, isoprostanes, and monohydroxylated metabolites. In this study, we report EETs as another important class of products readily formed from AA autoxidation. Non-enzymatic *trans*-EETs are formed more favorably via free radical oxidation mechanisms, while CYP epoxygenases contribute to the formation of *cis*-EETs. A number of studies have measured EETs in plasma of cardiovascular disease patients compared to healthy volunteers, however, future efforts should focus on determining if one (or more) geometric isomer is more likely to vary during cardiovascular disease. In this manner, the contribution of both free radical and enzymatic oxidation to the total circulating EET pool can be assessed leading to a better understanding of the protective roles played by each regioisomer, and establishing whether certain regio- or geometric- isomers can serve as potential biomarkers for specific cardiovascular conditions.

Funding

This work was supported in part by National Institute of Health Grants R01HL130880, R01HL088456 and R01HL096706 to R.A.T and National Science Foundation CHE-1664851 to L.X.

Author contributions

T.A. and B.S.R designed and performed experiments, analyzed and interpreted data, wrote and edited manuscript. R.N.L, N.S, and S.A.G provided samples, designed experiments and edited manuscript. L.X. and R.A.T provided materials, designed experiment, interpreted data, wrote and edited manuscript.

Competing interests

The authors declare that there is no conflict of interest.

Data and materials availability

Data are available upon request to the corresponding author.

One sentence summary

Free radical oxidation favors *cis*-over *trans*-EETs, while *in vivo* *cis*- are either higher or equal to *trans*-EETs in RBC and heart tissue of mice and humans.

Acknowledgments

The authors thank Dr. Nahush A. Mokadam from the Division of Cardiothoracic surgery at University of Washington and Dr. Jean C. Dinh from Children's Mercy Hospital for establishing our human heart bank, Dale Whittington and J. Scott Edgar for their expertise and assistance in mass spectrometric analysis.

References

- [1] H. Ying, L. Xu, N.A. Porter, Free radical lipid peroxidation: mechanisms and analysis. *Chem. Rev.* 111(10) (2011) 5944-72. <http://doi.org/10.1021/cr200084z> (PubMed PMID: 21861450)
- [2] L. Xu, N.A. Porter, Free radical oxidation of cholesterol and its precursors: Implications in cholesterol biosynthesis disorders, *Free Radic. Res.* 49(7) (2015) 835–849. <http://doi.org/10.3109/10715762.2014.985219> (PubMed PMID: 25381800)
- [3] B. Shao, J.W. Heinecke, HDL, lipid peroxidation, and atherosclerosis. *J. Lipid Res.* 50 (4) (2009) 599-601. <http://doi.org/10.1194/jlr.E900001-JLR200> (PubMed PMID: 19141435)
- [4] D. T. Lucas, L. I. Szweda, Cardiac reperfusion injury: aging, lipid peroxidation, and mitochondrial dysfunction. *Proc. Natl. Acad. Sci. U.S.A.* 95(2) (1998) 510-514. (PubMed PMID: 9435222)
- [5] G. Davi, A. Falco, C. Patrono, Lipid peroxidation in diabetes mellitus. *Antioxid. Redox Signal.* 7(1-2) (2005) 256-268. <http://doi.org/10.1089/ars.2005.7.256> (PubMed PMID: 15650413)
- [6] G. Barrera, Oxidative stress and lipid peroxidation products in cancer progression and therapy. *ISRN Oncol.* 2012 (2012) 137289. <http://doi.org/10.5402/2012/137289> (PubMed PMID: 23119185)
- [7] R. Abeti, M.H. Parkinson, I. P. Hargreaves, P.R. Angelova, C. Sandi, M.A. Pook, P. Giunti, A.Y. Abramov, Mitochondrial energy imbalance and lipid peroxidation cause cell death in Friedreich's ataxia. *Cell Death Dis.* 7 (2016) e2237. <http://doi.org/10.1038/cddis.2016.111> (PubMed PMID: 27228352)
- [8] E.H. Oliw, F.P. Guengerich, J.A. Oates, Oxygenation of arachidonic acid by hepatic monooxygenases. Isolation and metabolism of four epoxide intermediates. *J. Biol. Chem.* 257 (7) (1982) 3771- 3781. (PubMed PMID: 6801052)
- [9] E.H. Oliw, Oxygenation of polyunsaturated fatty acids by cytochrome P450 monooxygenases. *Prog. Lipid Res.* 33(3) (1994) 329-354. (PubMed PMID: 8022846)
- [10] L. Yang, K. Maki-Petaja, J. Cheriyan, C. McEniry, L.B. Wilkinson, The role of epoxyeicosatrienoic acids in the cardiovascular system. *Br. J. Clin. Pharmacol.* 80(1) (2015) 28-44. <http://doi.org/10.1111/bcp.12603> (PubMed PMID: 25655310)
- [11] S.N. Batchu, E. Law, D.R. Brocks, J.R. Falck, J.M. Seubert, Epoxyeicosatrienoic acid prevents postischemic electrocardiogram abnormalities in an isolated heart model. *J. Mol. Cell. Cardiol.* 46(1) (2009) 67-74. <http://doi.org/10.1016/j.yjmcc.2008.09.711> (PubMed PMID: 18973759)

[12] H. Jiang, J.C. McGiff, J. Quilley, D. Sacerdoti, L.M. Reddy, J.R. Falck, F. Zhang, K.M. Lerea, P.Y. Wong, Identification of 5,6-trans-epoxyeicosatrienoic acid in the phospholipids of red blood cells. *J. Biol. Chem.* 279(35) (2004) 36412-36418. <http://doi.org/10.1074/jbc.M403962200> (PubMed PMID: 15213230)

[13] H. Jiang, A.G. Zhu, M. Mamczur, C. Morisseau, B.D. Hammock, J.R. Falck, J. C. McGiff, Hydrolysis of cis- and trans- epoxyeicosatrienoic acids by rat red blood cells. *J. Pharmacol. Exp. Ther.* 326(1) (2008) 330-337. <http://doi.org/10.1124/jpet.107.134858> (PubMed PMID: 18445784)

[14] H. Jiang, J. Quilley, A.B. Doumad, A.G. Zhu, J.R. Falck, B. D. Hammock, C.T. Stier, Jr., M.A. Carroll, Increases in plasma trans-EETs and blood pressure reduction in spontaneously hypertensive rats. *Am. J. Physiol. Heart Circ. Physiol.* 300(6) (2011) H1990-H1996. <http://doi.org/10.1152/ajpheart.01267.2010> (PubMed PMID: 21398593)

[15] T. Nakamura, D.L. Bratton, R.C. Murphy, Analysis of epoxyeicosatrienoic and monohydroxyeicosatetraenoic acids esterified to phospholipids in human red blood cells by electrospray tandem mass spectrometry. *J. Mass Spectrom.* 32(8) (1997) 888-896. [http://doi.org/10.1002/\(SICI\)1096-9888\(199708\)32:8<888::AID-JMS548>3.0.CO;2-W](http://doi.org/10.1002/(SICI)1096-9888(199708)32:8<888::AID-JMS548>3.0.CO;2-W) (PubMed PMID: 9269087)

[16] H. Jiang, G.D. Anderson, J.C. McGiff, Red blood cells (RBCs), epoxyeicosatrienoic acids (EETs) and adenosine triphosphate (ATP). *Pharmacol. Rep.* 62(3) (2010) 468-474. (PubMed PMID: 20631410)

[17] L. Xu, T.A. Davis, N.A. Porter, Rate constants for peroxidation of polyunsaturated fatty acids and sterols in solution and in liposomes. *J. Am. Chem. Soc.* 131(36) (2009) 13037-13044. <http://doi.org/10.1021/ja9029076> (PubMed PMID: 19705847)

[18] D.S. Siscovick, T.E. Raghunathan, I. King, S. Weinmann, K.G. Wicklund, J. Albright, V. Bovbjerg, P. Arbogast, H. Smith, L.H. Kushi, L.A. Cobb, M.K. Copass, B.M. Psaty, R. Lemaitre, B. Retzlaff, M. Childs, R.H. Knopp, Dietary intake and cell membrane levels of long-chain n-3 polyunsaturated fatty acids and the risk of primary cardiac arrest. *JAMA*. 274(17) (1995) 1363-1367. (PubMed PMID: 7563561)

[19] S. Goulitquer, Y. Dreano, F. Berthou, L. Corcos, D. Lucas, Determination of epoxyeicosatrienoic acids in human red blood cells and plasma by GC/MS in the NICI mode. 876(1) (2008) 83-88. <http://doi.org/10.1016/j.jchromb.2008.10.035> (PubMed PMID: 19004672)

[20] E.A. Evangelista, R. Kaspera, N.A. Mokadam, J.P. Jones 3rd, R.A. Totah, Activity, inhibition, and induction of cytochrome P450 2J2 in adult human primary cardiomyocytes.

Drug Metab. Dispos. 41(12) (2013) 2087-2094. <http://doi.org/10.1124/dmd.113.053389> (PubMed PMID: 24021950)

- [21] R. Kaspera, R.A. Totah, Epoxyeicosatrienoic acids: formation, metabolism and potential role in tissue physiology and pathophysiology. Expert Opin. Drug Metab. Toxicol. 5(7) (2009) 757-771. <http://doi.org/10.1517/17425250902932923> (PubMed PMID: 19505190)
- [22] U. Roy, O. Loreau, M. Balazy, Cytochrome P450/NADPH-dependent formation of trans epoxides from trans-arachidonic acids. Bioorg. Med. Chem. Lett. 14(4) (2004) 1019-1022. <http://doi.org/10.1016/j.bmcl.2003.11.054> (PubMed PMID: 15013014)
- [23] H. Jiang, N. Kruger, D.R. Lahiri, D. Wang, J.M. Vatele, M. Balazy, Nitrogen dioxide induces cis-trans-isomerization of arachidonic acid within cellular phospholipids. Detection of trans-arachidonic acids in vivo. J. Biol. Chem. 274(23) (1999) 16235-16241. (PubMed PMID: 10347179)
- [24] C. Ferreri, A. Samadi, F. Sassatelli, L. Landi, C. Chatgilialoglu, Regioselective cis-trans isomerization of arachidonic double bonds by thiyl radicals: the influence of phospholipid supramolecular organization. J. Am. Chem. Soc. 126(4) (2004) 1063-1072. <http://doi.org/10.1021/ja038072o> (PubMed PMID: 14746474)
- [25] A.D.N. Vaz, D.F. McGinnity, M.J. Coon, Epoxidation of olefins by cytochrome P450: evidence from site-specific mutagenesis for hydroperoxo-iron as an electrophilic oxidant. Proc. Natl. Acad. Sci. U.S.A. 95 (7) (1998) 3555-3560. (PubMed PMID: 9520404)
- [26] L.H. Long, B. Halliwell, Artefacts in cell culture: pyruvate as a scavenger of hydrogen peroxide generated by ascorbate or epigallocatechin gallate in cell culture media. Biochem. Biophys. Res. Commun. 388(4) (2009) 700-704. <http://doi.org/10.1016/j.bbrc.2009.08.069> (PubMed PMID: 19695227)